

# Supplementary information for manuscript

## Evaporation of sulphate aerosols at low relative humidity

Georgios Tsagkogeorgas<sup>1</sup>, Pontus Roldin<sup>2,3</sup>, Jonathan Duplissy<sup>2,4</sup>, Linda Rondo<sup>5</sup>, Jasmin Tröstl<sup>6</sup>, Jay G.  
Slowik<sup>6</sup>, Sebastian Ehrhart<sup>5,a</sup>, Alessandro Franchin<sup>2</sup>, Andreas Kürten<sup>5</sup>, Antonio Amorim<sup>7</sup>, Federico  
5 Bianchi<sup>2</sup>, Jasper Kirkby<sup>5,8</sup>, Tuukka Petäjä<sup>2</sup>, Urs Baltensperger<sup>6</sup>, Michael Boy<sup>2</sup>, Joachim Curtius<sup>5</sup>,  
Richard C. Flagan<sup>9</sup>, Markku Kulmala<sup>2,4</sup>, Neil M. Donahue<sup>10</sup>, Frank Stratmann<sup>1</sup>

<sup>1</sup>Leibniz Institute for Tropospheric Research, 04318, Leipzig, Germany

<sup>2</sup>Department of Physics, University of Helsinki, P.O. Box 64, 00014, Helsinki, Finland

<sup>3</sup>Division of Nuclear Physics, Lund University, P.O. Box 118, 221 00, Lund, Sweden

10 <sup>4</sup>Helsinki Institute of Physics, University of Helsinki, P.O. Box 64, 00014 Helsinki, Finland

<sup>5</sup>Institute for Atmospheric and Environmental Sciences, Goethe University Frankfurt, 60438, Frankfurt am Main, Germany

<sup>6</sup>Paul Scherrer Institute, CH-5232, Villigen, Switzerland

<sup>7</sup>Fac. Ciências & CENTRA, Universidade de Lisboa, Campo Grande, 1749-016, Lisboa, Portugal

<sup>8</sup>CERN, CH-1211, Geneva, Switzerland

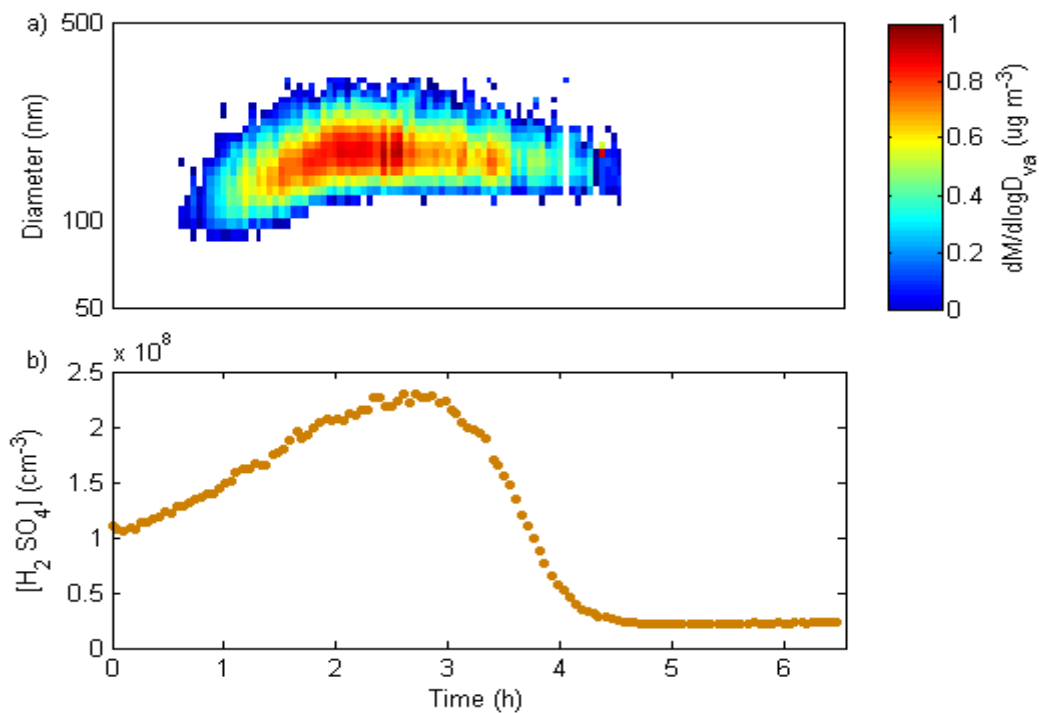
15 <sup>9</sup>California Institute of Technology, Pasadena, CA 91125, USA

<sup>10</sup>Center for Atmospheric Particle Studies, Carnegie Mellon University, Pittsburgh, PA 15213, USA

<sup>a</sup>now at: Atmospheric Chemistry Department, Max Planck Institute for Chemistry, 55128, Mainz, Germany

## S1 AMS measurements

The evaporation of particles based on AMS measurements showed that the particles were composed almost exclusively of sulphuric acid. Calculations of the kappa value  $\kappa$ , based on the AMS measurements, yield a value close to the  $\kappa$  for pure sulphuric acid particles (see Fig. S2).

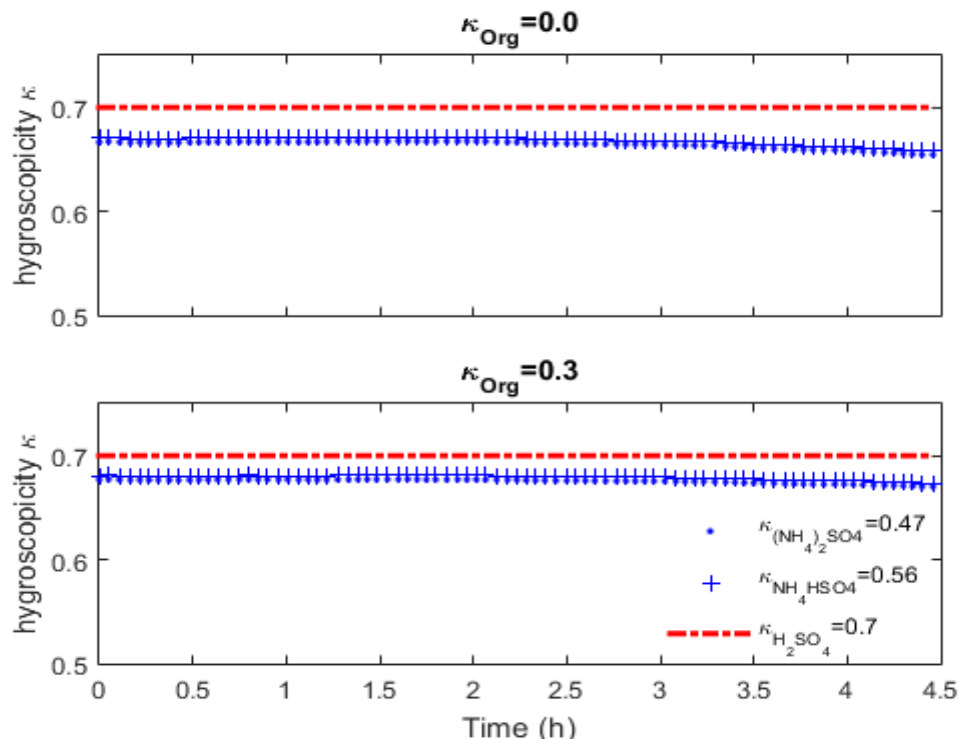


5

**Figure S1. (a) Sulphate mass size distribution  $\mu\text{g}\cdot\text{m}^{-3}$  (from AMS data) and (b) gas-phase  $\text{H}_2\text{SO}_4$  concentration (from CIMS data) increases until reaches a peak value during the aerosol particle evaporation experiment 2 performed at  $T=288.8 \text{ K}$ .**

10

15



5 Figure S2. Hygroscopicity kappa ( $\kappa$ ), based on the AMS measurements, of mixed particles as a function of time for experiment 3.  $\kappa$  derived from the hygroscopicities of the components (assumed the lower and higher  $\kappa$  values for bases like ammonium sulphate,  $\kappa_{(\text{NH}_4)_2\text{SO}_4}=0.47$  and ammonium bisulfate,  $\kappa_{\text{NH}_4\text{HSO}_4}=0.56$  (Topping et al., 2005; Petters and Kreidenweis 2007), and organics with  $O:C=0$ ,  $\kappa_{\text{Org}}=0.0$  and  $O:C=1$ ,  $\kappa_{\text{Org}}=0.3$  (Massoli et al., 2010)) and their respective volume fractions by applying the Zdanovskii–Stokes–Robinson (ZSR) mixing rule. For the calculation of the volume concentration of each compound assumed liquid phase density of  $\text{SO}_4$ ,  $\text{NH}_4$ ,  $\text{NO}_3$ ,  $\text{Chl}$ ,  $\text{Org}$  constituents (<http://cires1.colorado.edu/jimenez-group/wiki>). The difference in percentage of  $\kappa$  values calculated for the two extreme cases of  $\kappa_{(\text{NH}_4)_2\text{SO}_4}=0.47$ ,  $\kappa_{\text{NH}_4\text{HSO}_4}=0.56$  is 0.4 %, while for  $\kappa_{\text{Org}}=0.0$  and  $\kappa_{\text{Org}}=0.3$  is 1 %. The result shows a  $\kappa$  very close to that of pure sulphuric acid (Sullivan et al., 2010).

## S2 Activity coefficients of H<sub>2</sub>SO<sub>4</sub> and SO<sub>3</sub> and water activity

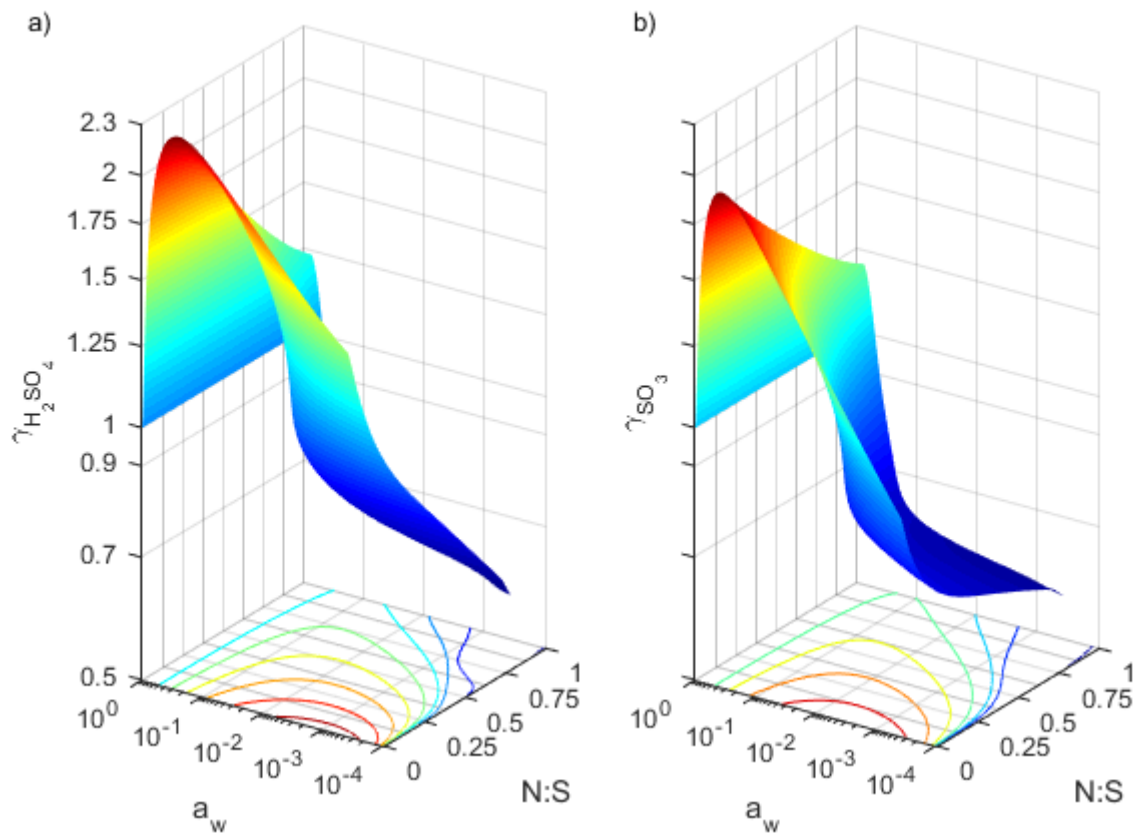


Figure S3. Modelled activity coefficient of (a) H<sub>2</sub>SO<sub>4</sub> ( $\gamma_{H_2SO_4}$ ) with equilibrium constant  $K_{H_2SO_4}=2.40 \cdot 10^9 \text{ mol} \cdot \text{kg}^{-1}$ , and (b) SO<sub>3</sub> ( $\gamma_{SO_3}$ ) with equilibrium constant  $^*K_{SO_3}=1.43 \cdot 10^{10}$ , at  $T=288.8 \text{ K}$ , as a function of the water activity,  $a_w$ , on the y-axis and N:S on the x-axis.

5 The colour coded contours on x-y axes represent constant activity coefficient for a)  $\gamma_{H_2SO_4}=0.8-2.2$  and b)  $\gamma_{SO_3}=0.8-1.8$ .

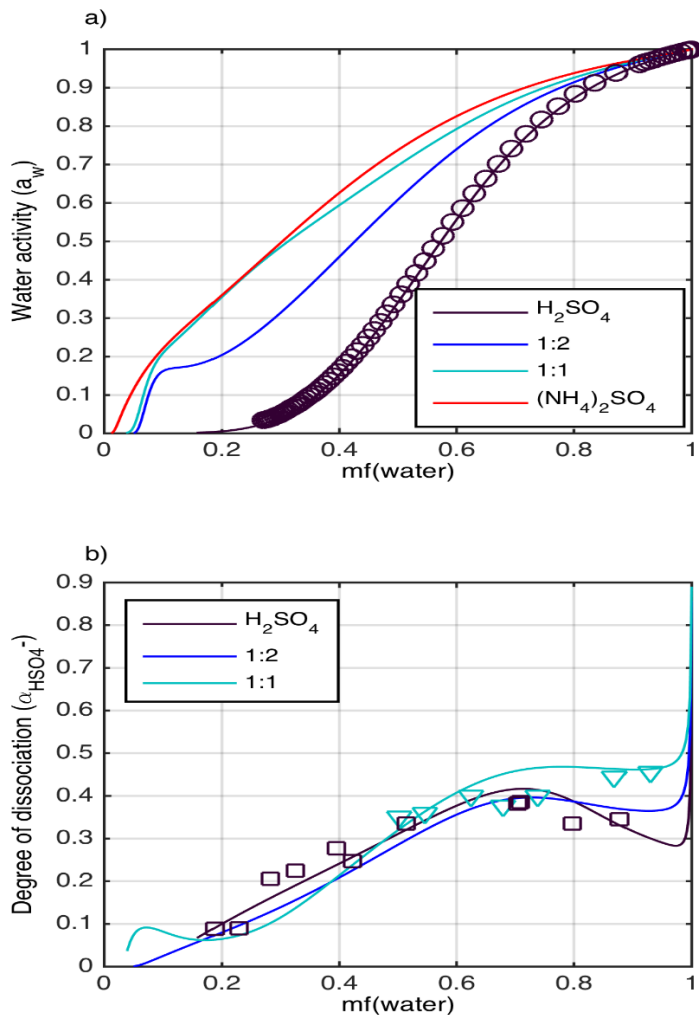
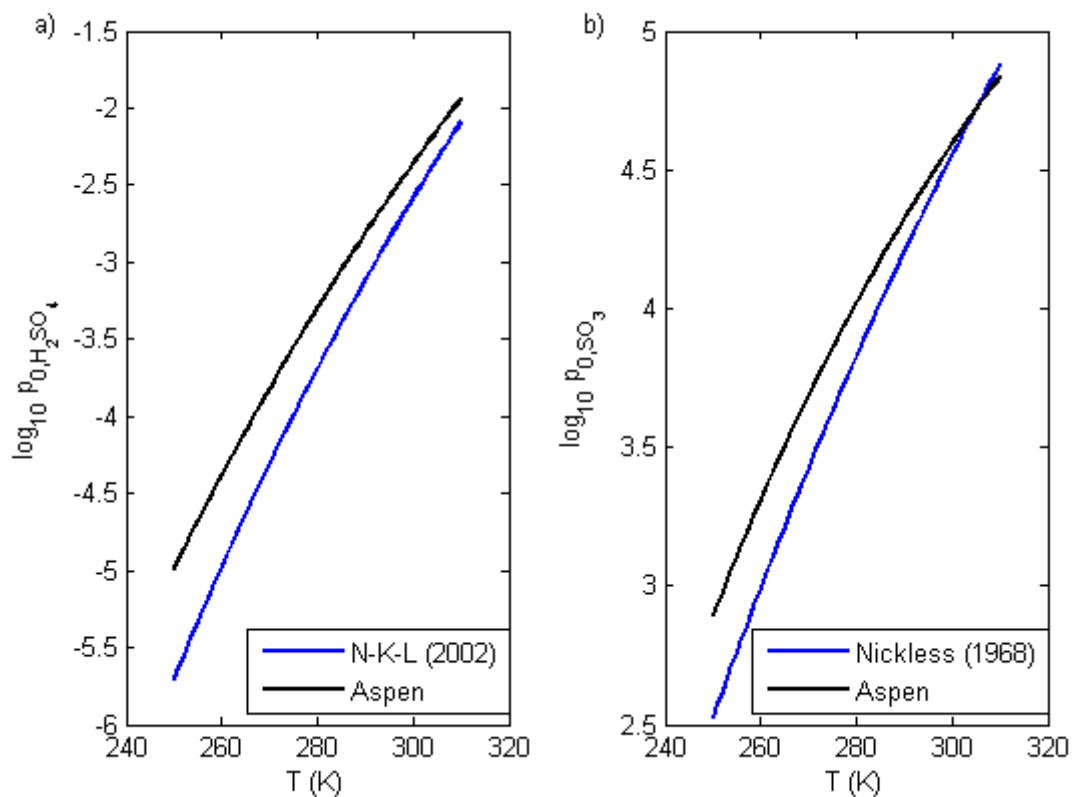


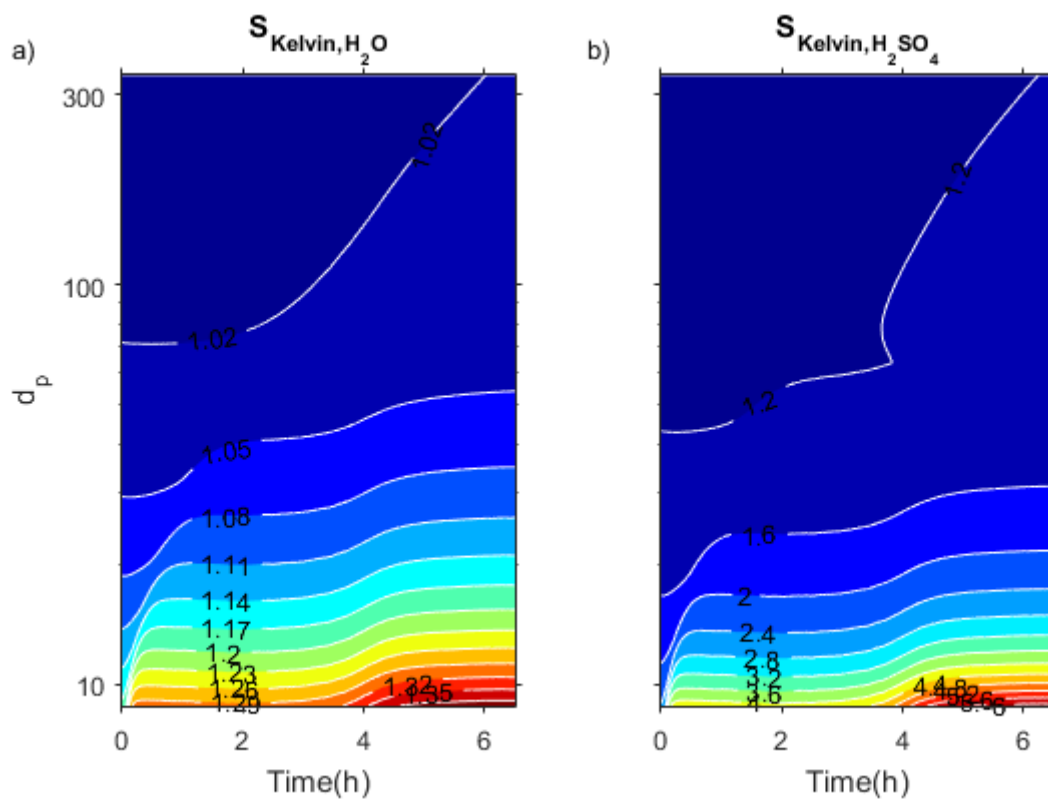
Figure S4. (a) Modelled water activity curves and (b) degree of dissociation of  $HSO_4^-$  as a function of water mass fraction in aqueous solutions of  $H_2SO_4$  and mixtures of  $(NH_4)_2SO_4$  and  $H_2SO_4$ . The model simulations and measurements were performed at 298 K. The modelled water activity curves are lines colour coded. The purple curve corresponds to pure sulphuric acid, blue and cyan curves to 1:2 and 1:1 molar ratio of  $(NH_4)_2SO_4:H_2SO_4$  and red curve to pure ammonium sulphate. The measured water activity curve is symbol coded. The purple circle symbol corresponds to  $H_2SO_{4(aq)}$  (Staples 1981). (b) the modelled degree of dissociation,  $\alpha_{HSO_4^-}$ , curves are lines colour coded (corresponding to same aqueous solutions as the curves in Fig. S4.a. The measured degree of dissociation is symbol colour coded (purple squares corresponds to  $H_2SO_{4(aq)}$ , Myhre et al. (2003), cyan triangles to the 1:1  $(NH_4)_2SO_4:H_2SO_4$  mixture, Dawson et al. (1986)). The model results can be compared with analogous results in Fig. 10 from Zuend et al., 2011.

### S3 Saturation vapour pressure parameterizations



5 **Figure S5. Saturation vapour pressures for  $\text{H}_2\text{SO}_4$  and  $\text{SO}_3$ . Comparison among two different pure liquid saturation vapour pressure parameterizations (a) for  $\text{H}_2\text{SO}_4$  and (b) for  $\text{SO}_3$ . In panel (a) the blue curve corresponds to the parameterization from the work of Kulmala and Laaksonen (1990), which was optimized by Noppel et al., 2002 (N-K-L). The black curve corresponds to the parameterization from Que et al., 2011 (original Aspen Plus Databank). In panel (b) the blue curve corresponds to the parameterization from the work of Nickless (1968) and the black curve to the parameterization from Que et al., 2011 (original Aspen Plus Databank).**

## S4 The Kelvin effect



5 **Figure S6.** The Kelvin effect for experiment 2 at  $T=288.8\text{ K}$  for Case 2a ( $K_{\text{H}_2\text{SO}_4}=2.40\cdot 10^9\text{ mol}\cdot\text{kg}^{-1}$  and  $K_{\text{SO}_3}=1.43\cdot 10^{10}$ ) illustrates the increase in (a) the water (white contours correspond to  $S_{\text{Kelvin}, \text{H}_2\text{O}}=1.02\text{--}1.38$ ) and (b) the  $\text{H}_2\text{SO}_4$  (white contours represent the Kelvin terms  $S_{\text{Kelvin}, \text{H}_2\text{SO}_4}=1.2\text{--}6.0$ ) saturation vapour pressure. The minimum particle size for experiment 2 is  $\sim 40\text{ nm}$ , so the maximum value of the Kelvin term is  $\sim 1.44$  for sulphuric acid.

## S5 Saturation concentration of H<sub>2</sub>SO<sub>4</sub> and SO<sub>3</sub>

We can calculate the saturation concentration of H<sub>2</sub>SO<sub>4</sub> ( $C_{H_2SO_4,S}$ , Eq.S1) and SO<sub>3</sub> ( $C_{SO_3,S}$ , Eq.S2) in  $\mu\text{g}\cdot\text{m}^{-3}$  (supplement Fig. S7) with the H<sub>2</sub>SO<sub>4</sub> dissociation equilibrium coefficients,  $K_{H_2SO_4}=2.4\cdot 10^9 \text{ mol}\cdot\text{kg}^{-1}$ , and  ${}^xK_{SO_3}=1.43\cdot 10^{10}$ , based on the mole fractions (Fig. 2), the modelled activity coefficients (Fig. S3), the pure liquid saturation vapours pressure parameterizations (Eq. 10 and 11), and the Kelvin effect (Eq. 13).

$$C_{H_2SO_4,S} = \frac{P_{0,H_2SO_4} \cdot x_{H_2SO_4} \cdot \gamma_{H_2SO_4} \cdot C_{k,H_2SO_4}}{R \cdot T \cdot M_{H_2SO_4}} \quad (\text{S1})$$

$$C_{SO_3,S} = \frac{P_{0,SO_3} \cdot x_{SO_3} \cdot \gamma_{SO_3} \cdot C_{k,SO_3}}{R \cdot T \cdot M_{SO_3}} \quad (\text{S2})$$

For almost dry conditions ( $a_w=3.7\cdot 10^{-4}$ ) and  $N:S=0$ ,  $C_{H_2SO_4,S}\approx 2.6 \mu\text{g}\cdot\text{m}^{-3}$  and  $C_{SO_3,S}\approx 8.8 \mu\text{g}\cdot\text{m}^{-3}$ . However, as long as  $a_w$  is larger than  $1.3\cdot 10^{-3}$ ,  $C_{H_2SO_4,S}$  becomes larger than  $C_{SO_3,S}$ . Thus, for the conditions during the experiments ( $RH>0.3\%$ ) this thermodynamic setup can be categorized as Case 2a.

With the Aspen Plus Databank pure–liquid saturation vapour pressure parameterization and  $K_{H_2SO_4}=4.00\cdot 10^9 \text{ mol}\cdot\text{kg}^{-1}$  and  ${}^xK_{SO_3}=4.55\cdot 10^{10}$   $C_{H_2SO_4,S}$  is always higher than  $C_{SO_3,S}$  ( $C_{H_2SO_4,S}=3.33 \mu\text{g}\cdot\text{m}^{-3}$  and  $C_{SO_3,S}=2.28 \mu\text{g}\cdot\text{m}^{-3}$  at  $a_w=2\cdot 10^{-4}$  and  $N:S=0$ ) (Fig. S7). Thus, this model setup can be also classified as Case 2a.



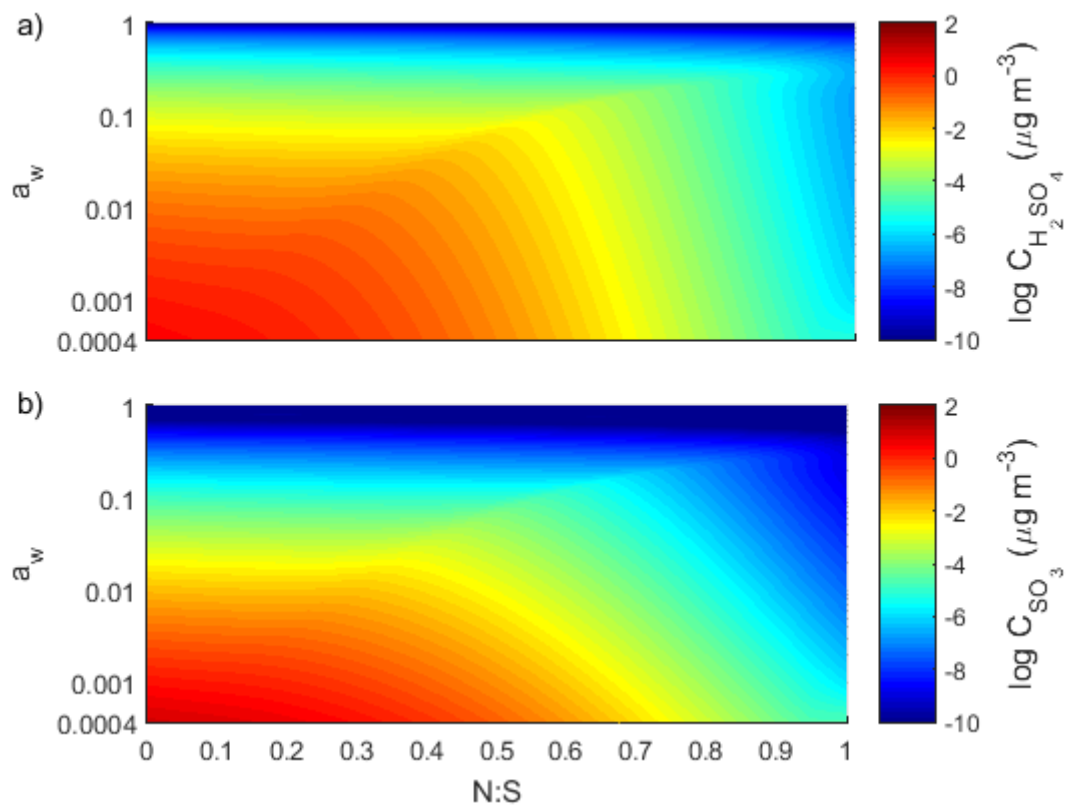
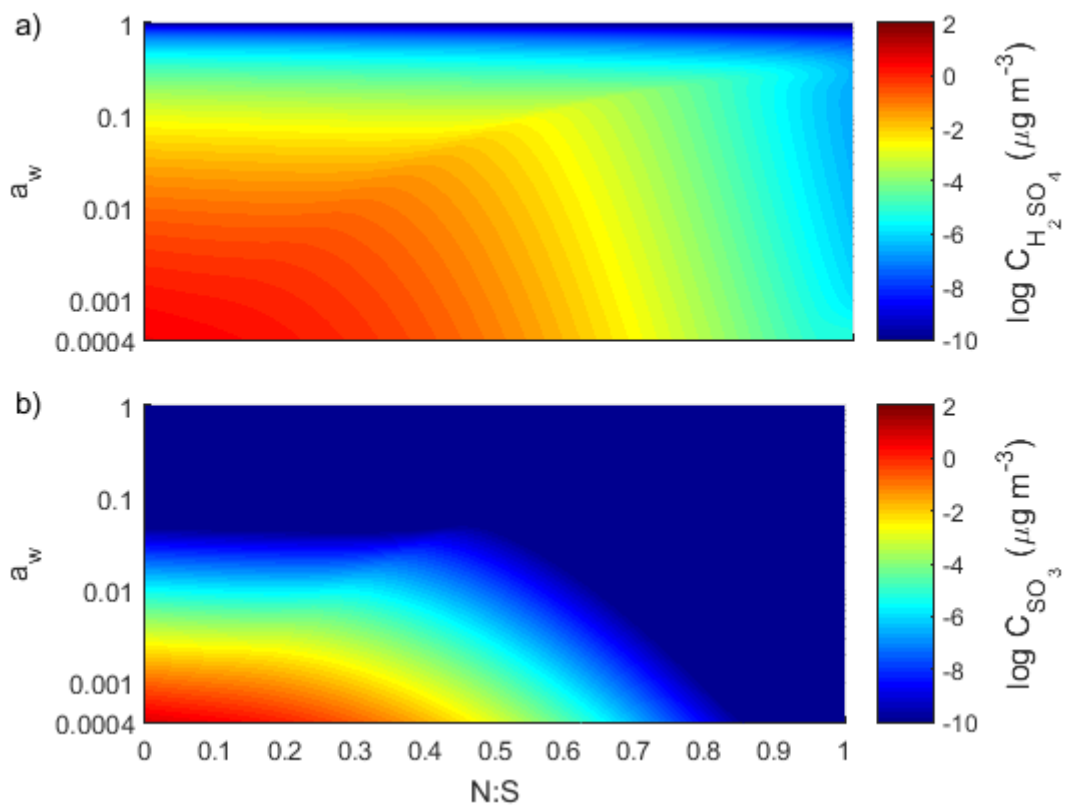


Figure S7.I. (a) The saturation concentration of H<sub>2</sub>SO<sub>4</sub> ( $C_{H_2SO_4,s}$ ) and (b) SO<sub>3</sub> ( $C_{SO_3,s}$ ) in  $\mu\text{g m}^{-3}$  as a function of  $a_w$  and N:S at  $T=288.8$  K. The H<sub>2</sub>SO<sub>4</sub> dissociation equilibrium coefficients are  $K_{H_2SO_4}=2.4\cdot 10^9 \text{ mol}\cdot\text{kg}^{-1}$ , and  ${}^xK_{SO_3}=1.43\cdot 10^{10}$ . For the pure liquid saturation vapour pressures used the N–K–L and Nickless parameterisations.



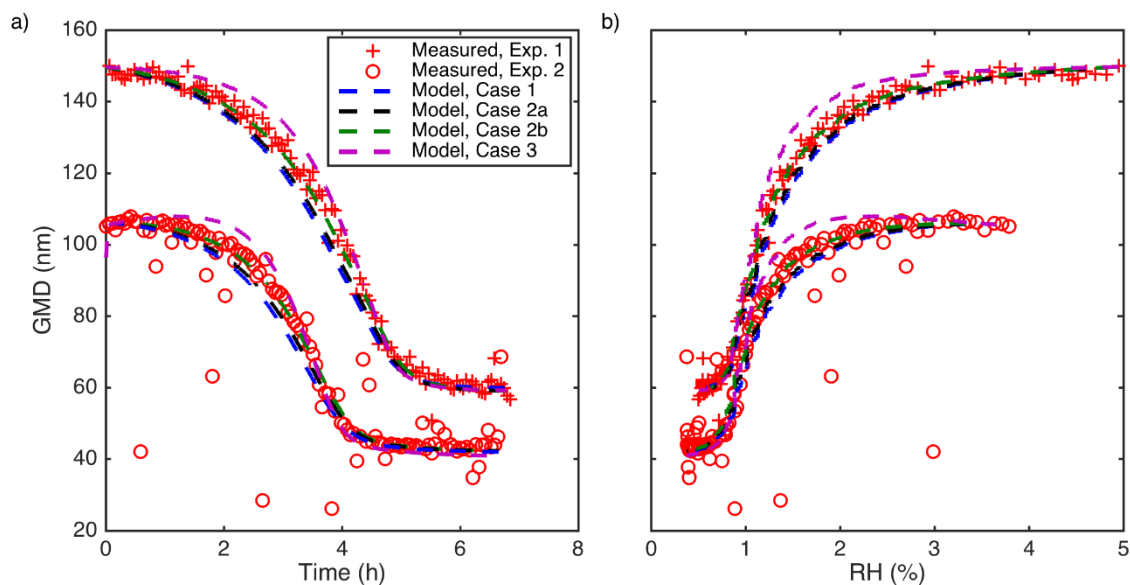
**Figure S7.II.** (a) The saturation concentration of  $\text{H}_2\text{SO}_4$  ( $C_{\text{H}_2\text{SO}_4}$ ) and (b)  $\text{SO}_3$  ( $C_{\text{SO}_3}$ ) in  $\mu\text{g}\cdot\text{m}^{-3}$  as a function of  $a_w$  and N:S at  $T=288.8$  K. The  $\text{H}_2\text{SO}_4$  dissociation equilibrium coefficients are  $K_{\text{H}_2\text{SO}_4}=4.00\cdot 10^9$  mol kg $^{-1}$ , and  ${}^xK_{\text{SO}_3}=4.55\cdot 10^{10}$ . For the pure liquid saturation vapour pressures used the parameterisations from Aspen Plus Databank.

5

10

15

## S6 Geometrical mean diameter



5 **Figure S8.** Modelled and measured GMD evolution as a function of (a) time and (b) RH for experiments 1 and 2 performed at  $T=288.8\text{ K}$ . The model results are from simulations 8–11 and 20–23 with  $\text{NH}_3$  as a particle phase contaminant listed in Table 2 (Case 1 ( $K_{\text{H}_2\text{SO}_4}=3.80\cdot 10^9\text{ mol}\cdot\text{kg}^{-1}$ ), Case 2a ( $K_{\text{H}_2\text{SO}_4}=4.00\cdot 10^9\text{ mol}\cdot\text{kg}^{-1}$  and  ${}^xK_{\text{SO}_3}=4.55\cdot 10^{10}$ ), Case 2b ( $K_{\text{H}_2\text{SO}_4}=5.00\cdot 10^9\text{ mol}\cdot\text{kg}^{-1}$  and  ${}^xK_{\text{SO}_3}=5.00\cdot 10^9$ ) and Case 3 ( $K_{\text{H}_2\text{SO}_4}=1.00\cdot 10^{11}\text{ mol}\cdot\text{kg}^{-1}$  and  ${}^xK_{\text{SO}_3}=5.00\cdot 10^7$ )). The pure liquid saturation vapour pressures of  $\text{H}_2\text{SO}_4$  and  $\text{SO}_3$  are calculated with the parameterizations from Que *et al.* (2011) (originally from the Aspen Plus Databank).

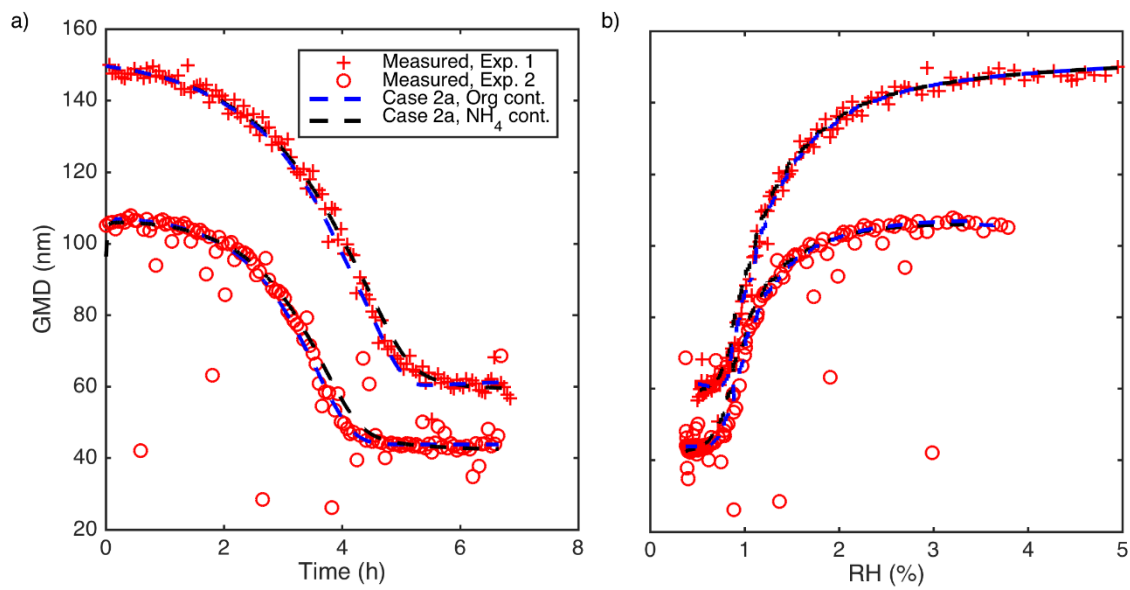


Figure S9. Modelled and measured GMD evolution as a function of (a) time and (b) RH for experiments 1 and 2 performed at  $T=288.8\text{ K}$ . The model results presented are from simulation 2, 6, 14 and 17 listed in Table 2 (Case 2a,  $K_{H_2SO_4}=2.40\cdot 10^9\text{ mol}\cdot\text{kg}^{-1}$  and  $^sK_{SO_3}=1.43\cdot 10^{10}$ ). The pure liquid saturation vapour pressures of  $H_2SO_4$  and  $SO_3$  are taken from Kulmala and Laaksonen (1990) (Eq. 10) and Nickless (1968) (Eq. 11), respectively. The only difference between the model simulations is the assumed particle contaminant ( $NH_3$  or non-volatile and non-water-soluble organics).

10

15

20

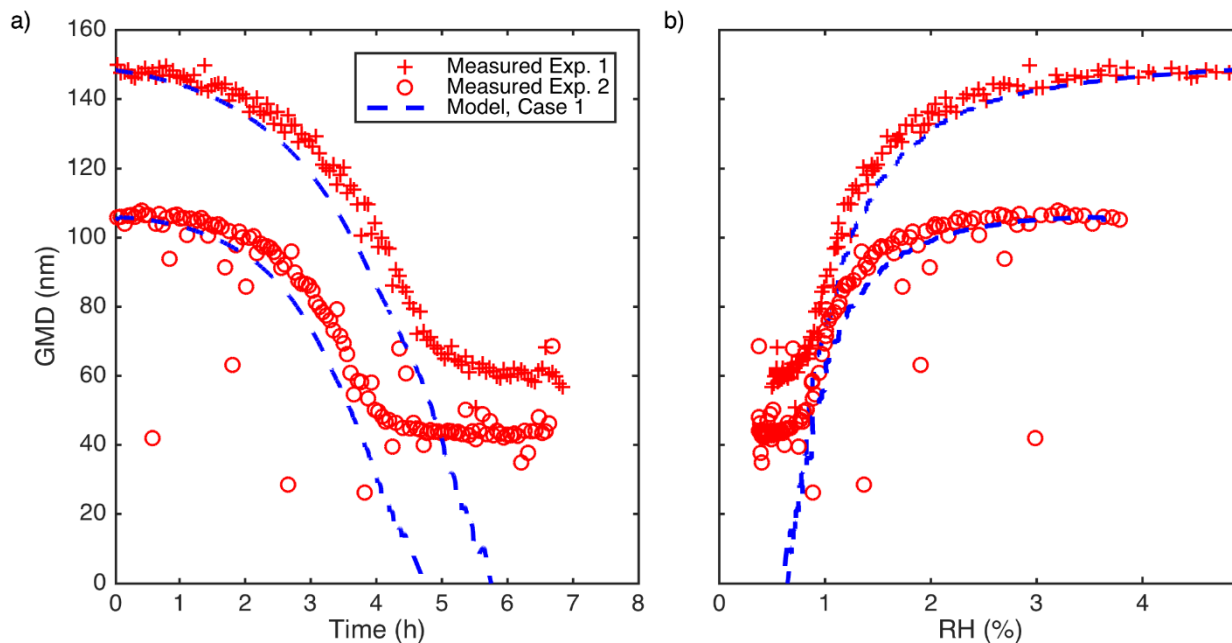


Figure S10. Modelled and measured GMD evolution as a function of (a) time and (b) RH for experiments 1 and 2 performed at  $T=288.8$  K. The model results presented arise from Case 1 simulations ( $K_{H_2SO_4}=2.00 \cdot 10^9 \text{ mol} \cdot \text{kg}^{-1}$ ) without any particle phase contaminant. The pure liquid saturation vapour pressures of  $H_2SO_4$  was calculated with Eq. 10, N-K-L parameterisation, (Kulmala and Laaksonen (1990) and Noppel et al., 2002).

5

10

15

## Supplementary references

- Dawson, B. S. W., Irish, D. E., and Toogood, G. E.: Vibrational spectral studies of solutions at elevated temperatures and pressures. 8. A Raman spectral study of ammonium hydrogen sulfate solutions and the hydrogen sulfate–sulfate equilibrium, *The Journal of Physical Chemistry*, 90 (2), 334–341, 1986.
- 5 Massoli, P., Lambe, A. T., Ahern, A. T., Williams, L. R., Ehn, M., Mikkila, J., Canagaratna, M. R., Brune, W. H., Onasch, T. B., Jayne, J. T., Petaja, T., Kulmala, M., Laaksonen, A., Kolb, C. E., Davidovits, P., and Worsnop, D. R.: Relationship between aerosol oxidation level and hygroscopic properties of laboratory generated secondary organic aerosol (SOA) particles, *Geophys. Res. Lett.*, 37, 5, L24801, 2010.
- Myhre, C. E. L., Christensen, D. H., Nicolaisen, F. M., Nielsen, C. J. Spectroscopic Study of Aqueous H<sub>2</sub>SO<sub>4</sub> at Different  
10 Temperatures and Compositions: Variations in Dissociation and Optical Properties. *J. Phys. Chem. A*, 107, 1979–1991, 2003.
- Petters, M. D. and Kreidenweis, S. M.: A single parameter representation of hygroscopic growth and cloud condensation nucleus activity, *Atmos. Chem. Phys.*, 7, 1961–1971, 2007.
- Staples, B. R.: Activity and Osmotic Coefficients of Aqueous Sulfuric Acid at 298.15 K, *J. Phys. Chem. Ref. Data*, 10, 779–798, 1981.
- 15 Sullivan, R. C., Petters, M. D., DeMott, P. J., Kreidenweis, S. M., Wex, H., Niedermeier, D., Hartmann, S., Clauss, T., Stratmann, F., Reitz, P., Schneider, J., and Sierau, B.: Irreversible loss of ice nucleation active sites in mineral dust particles caused by sulphuric acid condensation, *Atmos. Chem. Phys.*, 10, 11471–11487, 2010.
- Topping, D. O., McFiggans, G. B., and Coe, H.: A curved multicomponent aerosol hygroscopicity model framework: Part 2–Including organic compounds, *Atmos. Chem. Phys.*, 5, 1223–1242, 2005.
- 20 Zuend, A., Marcolli C., Booth, A. M., Lienhard, D. M., Soonsin, V., Krieger, U. K., Topping, D. O., McFiggans G., Peter, T., and Seinfeld, J. H.: New and extended parameterization of the thermodynamic model AIOMFAC: calculation of activity coefficients for organic–inorganic mixtures containing carboxyl, hydroxyl, carbonyl, ether, ester, alkenyl, alkyl, and aromatic functional groups, *Atmos. Chem. Phys.*, 11, 9155–9206, 2011.